

# Development of large-area, reverse-type APD arrays for high-resolution medical imaging

J. Kataoka<sup>a</sup>, M. Koizumi<sup>a</sup>, S. Tanaka<sup>a</sup>, H. Ishibashi<sup>a</sup>, T. Nakamori<sup>a</sup>, N. Kawai<sup>a</sup>, H. Ikeda<sup>b</sup>,  
Y. Ishikawa<sup>c</sup>, N. Kawabata<sup>c</sup>, Y. Matsunaga<sup>c</sup>, S. Kishimoto<sup>d</sup>, and H. Kubo<sup>e</sup>,

<sup>a</sup>*Tokyo Institute of Technology, 2-12-1 Ookayama, Meguro, Tokyo, 152-8551, Japan*

<sup>b</sup>*Institute of Space and Astronautical Science, JAXA, Sagami-hara, Kanagawa, Japan*

<sup>c</sup>*Solid State Division, Hamamatsu Photonics K.K., Hamamatsu, Shizuoka, Japan*

<sup>d</sup>*High Energy Accelerator Research Organization, Photon Factory, Tsukuba, Japan*

<sup>e</sup>*Department of Physics, Kyoto University, Sakyo-ku, Kyoto, Japan*

---

## Abstract

Avalanche photodiodes (APD) offer advantages in terms of weak scintillation detection, fast time response, and magnetic field insensitivity. We have developed new types of large-area, reverse-type APD arrays specifically designed for high resolution positron emission tomography (PET). Each device has a monolithic 16x16 (or 8x8) pixel structure with an active area of 1.0 (or 4.0, 0.25) mm<sup>2</sup> for each pixel. We have confirmed excellent gain uniformity ( $\leq 10\%$ ) and low dark-noise ( $\leq 0.3$  nA) measured at room temperature. Energy resolution of 7.2 % (FWHM) was obtained for the direct detection of 5.9 keV X-rays, while 10.2 % (FWHM) was obtained for 662 keV gamma-rays when coupled with a LYSO scintillator matrix. An excellent time resolution of 102 ps (FWHM) was obtained for a monolithic, 3 mm $\phi$  APD pixel. These results suggest that APD arrays could be a promising device for future applications in nuclear medicine.

*Key words:* avalanche photodiode,  $\gamma$ -rays, scintillation detection

*PACS:* 07.85; 87.57.uk; 87.57.U-

---

## 1. Introduction

The avalanche photodiode (APD) is a compact, high-performance light-sensor recently applied in various fields of experimental physics. In particular, the reverse-type APD offers great advantages in detecting weak light scintillation signals, thanks to its narrow high-field multiplying region close to the front end.[1-3] Moreover, this type of APD works at relatively low bias voltage (300–400 V) and achieves excellent noise characteristics. Unfortunately, only a single device (S8550; a monolithic 8 $\times$ 4 pixel structure with an active area of 2.56 mm<sup>2</sup> for each pixel) is now commercially available for application to high-resolution scintillator matrices readout.[4] This paper reports on the development of new types of large-area reverse-type APD arrays, specifically designed for future use in a APD-based PET (positron emission tomography) scanner.

PET scanners are powerful tools used for the study of physiological processes in vivo. Current developments aim at building smaller, and less expensive devices with improved image resolution (matching the sub-mm level or better [5]). The recent onset of using dual modality PET/CT imaging has had a profound effect on clinical diagnosis in radiology, oncology and other areas of nuclear medicine. However, CT exhibits a poor soft-tissue contrast, and also subjects the patient to a significant radiation dose exceeding that received from PET itself. In contrast, magnetic resonance imaging (MRI) provides an excellent soft-tissue contrast and anatomical detail, without an additional radiation dose. In this sense, APD is of great interest because it is insensitive to the high magnetic field used in the MRI ( $\sim 5$  T [6],[7]). Another important challenge for future PET detectors will be met by using time-of-flight (TOF) information to reduce statistical noise variance in the reconstructed image.[8]

With these motivations in mind, we began fabricating a simple PET device consisting of an APD-array optically coupled with a LYSO scintillator. The signals from each

---

\* Corresponding author. Tel.: +81-3-5734-2388; fax: +81-3-5734-2388

*Email address:* kataoka@hp.phys.titech.ac.jp (J. Kataoka).

pixel are read-out by a low-noise analog front-end ASIC specifically designed for the device.[9] This paper is organized as follows. Section 2 summarizes the basic properties of the newly developed APD-arrays. Section 3 presents the performance of APD-arrays in the direct detection of soft X-ray photons, as well as in the read-out LYSO matrix. We also demonstrate the excellent time response of a reverse-type APD using a monolithic pixel, for future application to the TOF-PET scanner. Finally, Section 4 presents our conclusion.

## 2. Newly developed APD-arrays

We have made three types of large-area, reverse-type APD arrays, that were developed based on the technology of the S8664 APD series (Hamamatsu). The basic characteristics of Hamamatsu APDs are documented in detail in other literature[1-3]. Table 1 lists the design parameters, dark noise and gain characteristic of each device. TYP1 carries an  $8\times 8$  array of  $2\times 2\text{ mm}^2$  pixels, while TYP2 and TYP3 consist of a  $16\times 16$  matrix of  $1\times 1\text{ mm}^2$  (TYP2) and  $0.5\times 0.5\text{ mm}^2$  (TYP3) pixels, respectively. As shown in Figure 1, all APD-arrays are embedded in a ceramic package of the same configuration,  $27.4\times 27.4\text{ mm}^2$  (1.27 mm pitch, pin-grid type)<sup>1</sup>. We tried to maximize the effective area of the APD for a given geometry. For example, the TYP1 array has 0.3 mm gaps between the  $2\times 2\text{ mm}^2$  pixels, compared to 0.7 mm gaps for the  $1.6\times 1.6\text{ mm}^2$  pixels of S8550, thereby improving the effective area of the APD from 48% (S8550) to 76 % (TYP1).

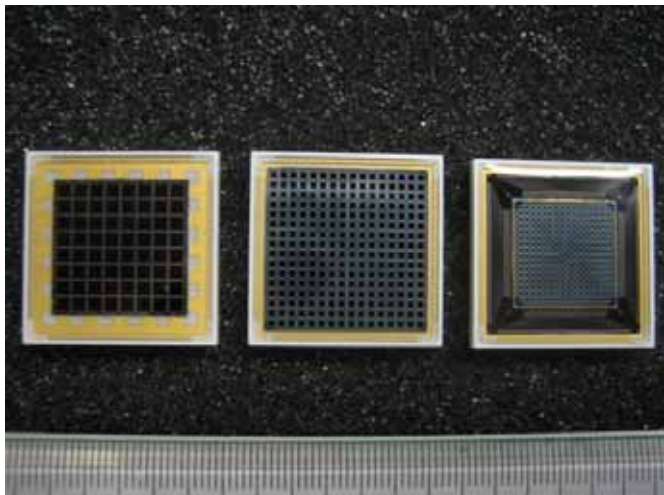


Fig. 1. A picture of the reverse APD-arrays developed in this paper. (TYP1 to 3; from left to right).

Our APD-arrays allow stable operations at gain up to 100, with extremely low dark-noise for each pixel, even at room temperature. An avalanche gain of 50 is achieved

<sup>1</sup> At this stage, the ceramic package was specifically designed to be matching with TYP2 array (Figure 1: center). We plan to make optimum packages also for TYP1 and TYP3 arrays in future fabrication to further reduce the dead space.

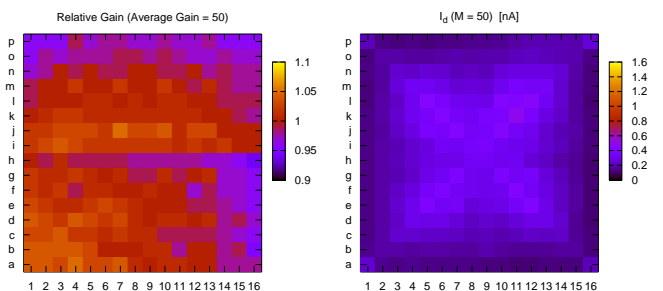


Fig. 2. Variation of APD gain (*left*) and dark current distribution (*right*) for the TYP2 array.

Table 1

Parameters of newly developed Hamamatsu APD-arrays.

|                               | TYP1                    | TYP2                    | TYP3                        |
|-------------------------------|-------------------------|-------------------------|-----------------------------|
| Matrix array                  | $8\times 8$             | $16\times 16$           | $16\times 16$               |
| Pixel size                    | $2\times 2\text{ mm}^2$ | $1\times 1\text{ mm}^2$ | $0.5\times 0.5\text{ mm}^2$ |
| Pixel gap                     | 0.3 mm                  | 0.4 mm                  | 0.4 mm                      |
| Dark current ( $M=50$ ) $I_D$ | 0.5-1.3 nA              | 0.1-0.3 nA              | 0.1-0.4 nA                  |
| Break-down voltage: $V_{brk}$ | 379 V                   | 376 V                   | 380 V                       |
| Operation bias: $V_{M=50}$    | 355 V                   | 333 V                   | 356 V                       |
| Capacitance: $C_{det}$        | 13-15 pF                | 4-5 pF                  | 3.3-4.6 pF                  |

All parameters are measured at  $+25^\circ\text{C}$ .

with a bias voltage of 330–360 V, which is sufficiently low compared to that required for other types of APDs (as described elsewhere [10]). Furthermore the APD gain shows excellent uniformity over the entire APD pixels. Figure 2 shows the gain variation (*left*) and dark noise distribution (*right*) for the TYP2 array, measured at gain  $M = 50$  and  $T = 25^\circ\text{C}$ . Note the excellent uniformity of avalanche gain. Gain fluctuation is only at the 10% level over the APD device. Dark noise is also uniform with an average of  $I_D = 0.23\pm 0.08\text{ nA/pixel}$  ( $1\text{ mm}^2$ ).

## 3. Detector Performance

### 3.1. Direct X-ray detection

To demonstrate the performance of our APD-arrays, the device was irradiated by a  $^{55}\text{Fe}$  source which emits 5.9 keV X-rays. Energy resolution of  $7.2\pm 0.6\%$  (FWHM) was obtained for all the APD pixels, representing one of the best records ever reported using APD devices (Figure 3). Thanks to the extremely low dark-noise, the energy threshold is as low as  $E_{th} \sim 0.6\text{ keV}$ , measured at room temperature ( $+25^\circ\text{C}$ ). One drawback is that, the device does not allow efficient X-ray detection due to its thin depletion layer ( $\sim 10\mu\text{m}$ ). For this particular purpose, thicker ( $\simeq 130\mu\text{m}$ ) reach-through APDs and beveled-edge APDs are more advantageous as discussed in other literature [10,11].

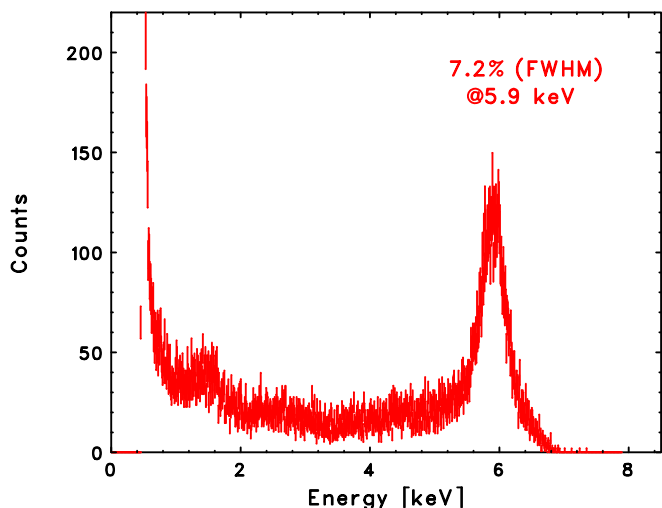


Fig. 3. An example of 5.9 keV X-ray spectrum measured with the TYP1 array.

### 3.2. Readout of LYSO scintillator matrix

Next we fabricated a prototype gamma-ray camera consisting of an APD-array optically coupled with a LYSO matrix. Figure 4 (*upper*) shows a picture of the 16×16 LYSO matrix for TYP2, where each pixel is  $1.3 \times 1.3 \times 10 \text{ mm}^3$  in size and divided with the lattice of a thin reflective layer (3M ESR). Figure 4 (*lower*) shows the TYP1 APD-array coupled with the LYSO matrix. In testing the proto-type, we used a low-noise analog front-end ASIC specifically designed for our APD-PET system.[9]. Figure 5 shows an example of an energy spectrum obtained with the TYP1+LYSO array (measured at  $+25^\circ\text{C}$ ) for the  $^{137}\text{Cs}$  source. The energy resolution of the 662 keV gamma-ray is  $10.2 \pm 0.2 \%$  (FWHM). The variation in signal amplitude (due to inhomogeneities of APD gain and LYSO light yield) was only  $\pm 16\%$  among  $8 \times 8$  pixels. A small peak in the spectrum (blue arrow) is due to the cross-talk of scintillation light from neighboring LYSO pixels through the epoxy window covering the APD surface. This low-level interference is actually acceptable for PET imaging, but a revised version of APD-arrays with a thin epoxy coating is being fabricated.

### 3.3. Time Response

Following a method described in other literature[12], a timing experiment on the reverse-type APD was carried out at the beamline NW2A of the PF-AR ring (KEK) at Tsukuba, Japan. In this experiment, we used a monolithic reverse-type APD pixel (S8664-30; Hamamatsu,  $3 \text{ mm } \phi$ ) to simplify the setup. Note that the internal structure of the S8664-30 is exactly the same as that of the APD-arrays, except for the pixel geometry. A double-crystal silicon (111) monochromator was used to define X-ray energy as 16 keV with an energy resolution of  $\Delta E \simeq 4 \text{ eV}$ . The X-ray beam was focused by a mirror into a spot size of  $0.7 \times 0.3$

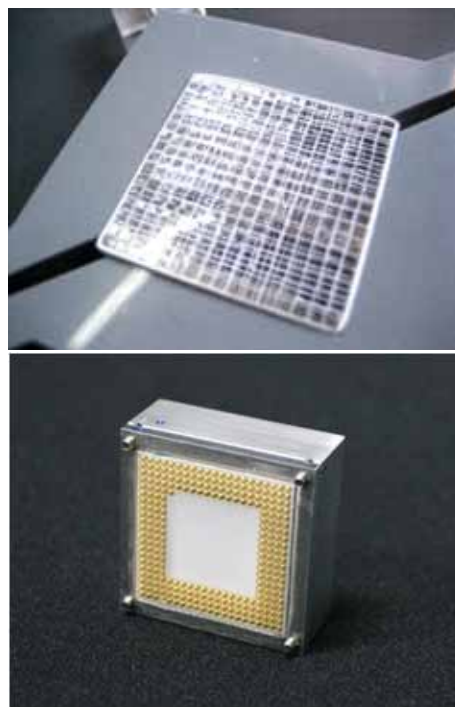


Fig. 4. (*upper*) A picture of the 16×16 LYSO matrix. (*lower*) The TYP2 APD-array coupled with a LYSO matrix.

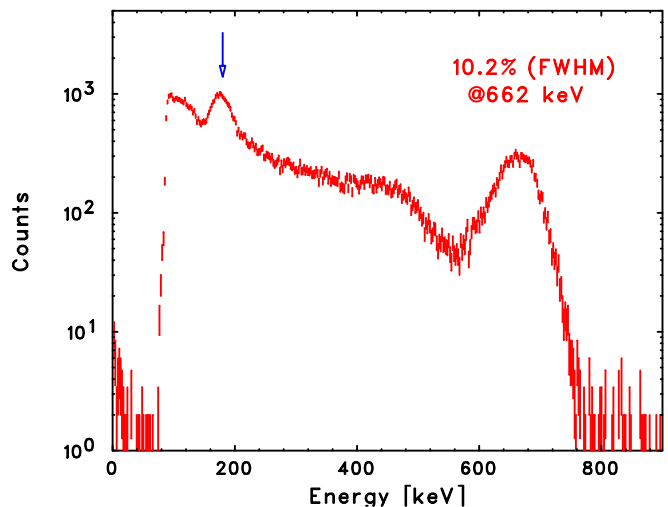


Fig. 5. An example of 662 keV gamma-ray spectrum obtained using the LYSO matrix coupled with the TYP1 APD-array.

$\text{mm}^2$ . Output signals from the APD were processed with a constant fraction discriminator (CFD: ORTEC 935) and fed into a time-to-amplitude converter (TAC: TENELEC TC863) with a maximum range of 50 ns, then finally digitized by an analog-to-digital converter (ADC) with 2048 ch resolution (25 ps/ch). During the experiment, the beam at PF-AR was operated in single-bunch mode.

Figure 6 shows the time response of the APD pixel as measured by the direct detection of 16 keV X-rays. The APD was operated under a bias voltage of 400 V, corresponding to an avalanche gain of  $\simeq 100$ . A measured time resolution from raw data provides  $\Delta T_{\text{all}} = 190 \text{ ps}$  (FWHM),

while most of the broadening is due to a width of electron bunches of the light source itself, and estimated as  $\Delta T_B = 160$  ps (FWHM). Hence the intrinsic time resolution of APD is expected to be  $\Delta T_{APD} = 102$  ps (FWHM). Note that this is much better than the timing response reported in literature. For example, the measured time resolution of  $3.0 \pm 0.2$  ns was obtained using the APD array S8550 (Hamamatsu) for 511 keV annihilation of the quanta from a  $^{22}\text{Na}$  source.[4] For measurement purposes, the APD was implemented with LSO scintillation pixels so that the time resolution is convolved not only for the APD-array but also for the LSO scintillator as well. Moreover, preamplifier response was not very fast, thereby worsening the time resolution. We showed that an *intrinsic* time resolution of the reverse-type APD is much better than previously thought, and future applications for TOF-PET are viable. The precise temporal measurement using a complete detector system (i.e., APD-array, LYSO, read-out ASIC) will be reported in the near future.

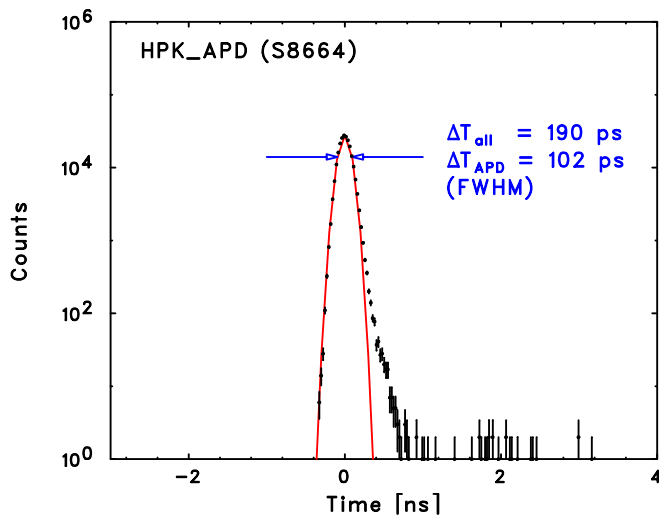


Fig. 6. Time response of the pixel APD S8664-30 measured with 16 keV X-rays.

#### 4. Conclusion

We have briefly overviewed the designs and performance of large-area APD-arrays recently developed with Hamamatsu Photonics K.K. Excellent gain uniformity ( $\leq 10\%$ ) and low dark-noise ( $\leq 0.3$  nA) characteristics were reported. Energy resolution of 7.2 % (FWHM) was obtained for the direct detection of 5.9 keV X-rays, while 10.2 % (FWHM) was obtained for 662 keV gamma-rays when coupled with a LYSO array. Excellent time resolution of 102 ps (FWHM) was also obtained using a 16 keV X-ray beam for monolithic reverse-type APD pixels. These results suggest that the newly developed APD arrays offer a promising device for future application in nuclear imaging, such as MRI/PET and the TOF-PET scanner.

#### References

- [1] T. Ikagawa, et al., Nucl. Instr. and Meth, A, 515 (2003) 671
- [2] J. Kataoka, et al., Nucl. Instr. and Meth, A, 541 (2005) 398
- [3] T. Ikagawa, et al., Nucl. Instr. and Meth, A, 538 (2003) 640
- [4] M. Kapusta et al., Nucl. Instr. and Meth, A, 504 (2003), 139
- [5] R. Lecomte, et al., Nucl. Instr. and Meth, A, 527 (2004) 157
- [6] J. Marler, et al., Nucl. Instr. and Meth, A, 449 (2000) 311
- [7] C. Woody et al., Nucl. Instr. and Meth, A, 571 (2007), 102,
- [8] W. W. Moses, Nucl. Instr. and Meth, A, 580 (2007), 919,
- [9] M. Koizumi, et al., Nucl. Instr. and Meth, A, (2008) in this volume
- [10] M. Moszyński, et al., IEEE Trans. Nucl. Sci., 49 (2002) 971
- [11] Y. Yatsu, et al., Nucl. Instr. and Meth, A, 564 (2006) 134
- [12] S. Kishimoto, et al., Nucl. Instr. and Meth, A, 513 (2003) 193